Int J Biometeorol
DOI 10.1007/s00484-016-1185-0

ORIGINAL PAPER

Methodology to estimate variations in solar radiation reaching densely forested slopes in mountainous terrain

Przemysław Sypka[1] · **Rafał Starzak**[2] · **Krzysztof Owsiak**[2]

Received: 31 May 2015 / Revised: 17 April 2016 / Accepted: 6 May 2016

Abstract Solar radiation reaching densely forested slopes is one of the main factors influencing the water balance between the atmosphere, tree stands and the soil. It also has a major impact on site productivity, spatial arrangement of vegetation structure as well as forest succession. This paper presents a methodology to estimate variations in solar radiation reaching tree stands in a small mountain valley. Measurements taken in three inter-forest meadows unambiguously showed the relationship between the amount of solar insolation and the shading effect caused mainly by the contour of surrounding tree stands. Therefore, appropriate knowledge of elevation, aspect and tilt angles of the analysed planes had to be taken into consideration during modelling. At critical times, especially in winter, the diffuse and reflected components of solar radiation only reached some of the sites studied as the beam component of solar radiation was totally blocked by the densely forested mountain slopes in the neighbourhood. The cross-section contours and elevation angles of all obstructions are estimated from a digital surface model including both digital elevation model and the height of tree stands. All the parameters in a simplified, empirical model of the solar insolation reaching a given horizontal surface within the research valley are dependent on the sky view factor (*SVF*). The presented simplified, empirical model and its parameterisation scheme should be easily adaptable to different complex terrains or mountain valleys characterised by diverse geometry or spatial orientation. The model was developed and validated ($R^2 = 0.92$, $\sigma = 0.54$) based on measurements taken at research sites located in the Silesian Beskid Mountain Range. A thorough understanding of the factors determining the amount of solar radiation reaching woodlands ought to considerably expand the knowledge of the water exchange balance within forest complexes as well as the estimation of site productivity.

Keywords Solar surface irradiance · Complex topography · Obstruction effect · Istebna spruce stand

Electronic supplementary material The online version of this article (doi:10.1007/s00484-016-1185-0) contains supplementary material, which is available to authorized users.

✉ Przemysław Sypka
sypka@agh.edu.pl

[1] Department of Electronics, AGH University of Science and Technology, Al. Mickiewicza 30, 30-056 Kraków, Poland

[2] Department of Forest Engineering, University of Agriculture in Krakow, Al. 29 Listopada 46, 31-425 Kraków, Poland

Introduction

A proper approximation of solar insolation on the Earth's surface is a fundamental issue in climate monitoring and in various hydrological and biological applications. Besides wind velocity and soil humidity, the solar energy reaching the soil surface in a forest is the main factor influencing the volume of water evaporating from inter-particle spaces in the soil. Furthermore, evaporation from soil is a fundamental factor affecting water exchange between the atmosphere, tree stands and the soil (Galicia et al. 1999; Wilson et al. 2000; Bouchter et al. 2001). The amount of photosynthetically active radiation (PAR) on canopies determines site productivity (Vose and Allen 1988), biomass and the spatial arrangement of foliage (Chen et al. 1997) and forest succession (Pons 2000; Piedallu and Gégout 2008). A habit of non-shaded trees is characterised by a wide, pyramidal crown. In contrast, trees in dense forest communities have narrow crowns and their canopy is lifted as a result of a strong self-pruning process due to light deficiency (Ediriweera et al. 2008). At the forest

Published online: 24 May 2016

floor, solar radiation has an impact on understory vegetation, variations in soil temperature (diurnal and seasonal) as well as various biological and chemical processes, such as decomposition and mineralisation (rotting) of soil organic matter (Dziadowiec et al. 2004). Growth rate is subject to changes in relative lengths of light and dark periods, which are highly dependent on latitude, time of year and the aspect and tilt angles of slopes in mountainous terrain. Photoperiodism is the controlling factor of flowering and fruit production, so in moderate climates, it is essential for perennial plants to prepare for winter, meaning termination of annual growth, lignification of shoots and shedding of leaves (Pons 2000). The influence of aspect and tilt angles on the forestation of slopes has been observed for many years (Puchalski and Prusinkiewicz 1975). Varying levels of solar insolation on a slope is a vital factor when modelling spatial arrangement of vegetation structure in forest complexes and potential for forest trees to grow at a particular location, described by the radiative aridity index or by the site quality index (Tajchman 1984).

Due to technical and organisational constraints of field research, solar radiation can only be measured at a few carefully chosen points at different heights. Furthermore, standard weather stations usually gauge total insolation at open, unobstructed areas with upward-looking sensors. Therefore, it is essential to convert obtained results to radiation on inclined surfaces with arbitrary aspect and tilt angles, α and β, respectively. The total radiation on a tilted plane I_β may be computed using the following formula (Liu and Jordan 1963):

$$I_\beta = R_b \cdot I_b + R_d \cdot I_d + R_r \cdot \rho_r \cdot (I_b + I_d) \quad (1)$$

where R_b is beam radiation tilt factor, the ratio of direct solar radiation falling on a tilted surface to that falling on a horizontal surface; I_b is the intensity of beam solar radiation on a horizontal surface [W m^{-2}]; R_d is diffuse radiation tilt factor, the ratio of radiation flux falling on an inclined surface to the diffuse radiation falling on a horizontal surface, with the diffuse tilt factor being proportional to the sky view factor; I_d is the intensity of diffuse solar radiation on a horizontal surface [W m^{-2}]; R_r is reflected radiation tilt factor; and ρ_r is albedo.

The simplest, Liu–Jordan method is most often used in practical research. This scheme assumes the isotropic character of the diffuse and reflected components of solar radiation. The isotropic model presupposes that the diffuse component is uniformly distributed over the sky and the diffuse irradiance is independent of direction. This is a reasonable approximation when there is a uniform cloud cover or when weather conditions are very hazy. More sophisticated models take into consideration the anisotropy of diffuse radiation and distinguish its two additional sub-components: circumsolar brightening and horizon brightening. Despite their more complicated mathematical forms, the final results are very similar to the Liu–Jordan model (Şen 2008).

When measurements are taken at open, unobstructed areas, the value of tilt factor for diffuse radiation may be calculated by the following formula:

$$R_d = \frac{1 + \cos\beta}{2} \quad (2)$$

where β is the tilt angle of an inclined surface. The value of the beam radiation tilt factor is evaluated based on the Hottel–Woertz algorithm (Duffie and Beckman 1991):

$$R_b = \frac{\cos\theta_\beta}{\cos\theta_h} \quad (3)$$

where θ_β is the incidence angle of the sun's rays on a tilted surface with an inclination angle of β and θ_h is the incidence angle of the sun's rays on a horizontal surface. The incidence angles of θ_β and θ_h change continuously over time; therefore, it is essential to know the precise position of the sun at a given moment.

Standard approaches usually focus on aspect and tilt angles of slopes and seldom, if ever, on the topographic relief of the surrounding terrain (Coops et al. 2000; Tian et al. 2001; Mayer et al. 2002; Holst et al. 2005; Holst and Mayer 2005; Yard et al. 2005; Wang et al. 2006; Promis et al. 2009). In a complex mountainous terrain, a temporary shading effect is the result not only of the topographic relief of adjoining mountain ranges, peaks and passes but above all the contour of neighbouring tree stands, this being an additional factor that has a major influence on observed and measured solar insolation. This paper presents the variations of solar insolation inside a densely forested small V-shaped mountain valley, which covers an area of 1.68 km^2. In such a small investigated area, the varying levels of solar radiation may only be a result of topographic factors and the outline of neighbouring tree stands. The main aim of the present study is to find and test a methodology for estimation of downward shortwave radiation in rugged, densely forested terrain. An additional objective is the expression of variations by means of topographical factors, as well as an attempt at physical interpretation of the obtained coefficients of the empirical model. This goal may be reached by estimating the obstruction effect caused by the topographic relief of adjoining mountain ranges and the contour of adjacent tree stands. Such empirical models which describe general relationships are crucial for forest practice. Estimation of solar insolation should be taken into consideration during choosing a type of cutting method (clear-cutting and selection systems) and spatial arrangement of openings, i.e. shape, size and location relative to neighbouring tree stands (Grayson et al. 2012). The presented methodology and the empirical model can be used to generate digital maps which may depict variations in solar radiation in complex terrain and considerably expand the capability for predicting

the results of silvicultural measures, estimation of site productivity as well as the growth conditions in regeneration areas.

Sites and measurements

The investigated sites were located inside the experimental catchment area Dupniański stream (49°35′N, 18°50′E) in the Silesian Beskid Mountain Range (Poland), where research on the water exchange balance between the atmosphere, tree stand and the soil of the Istebna spruce stands was carried out. The experimental drainage basin was organised by the Department of Forest Engineering at the University of Agriculture in Krakow. This small, mountain catchment (total area of 1.68 km^2) was 95 % covered by a Norway spruce stand (*Picea abies* (L) Karst., the Istebna ecotype). Eighteen research sites were located inside the experimental catchment. The spatial arrangement of all research sites inside the Dupniański stream catchment is presented in Fig. 1. Due to the fact that the catchment was densely forested and the height of tree stands in the research plot was usually higher than 16 m, all measurements of total solar insolation were taken at only three sites located in inter-forest meadows (sites S5, M1 and M2, Table 1). The other sites, situated within tree stands and denoted by capital letters, were used as points with arbitrary chosen aspect and tilt angles, where solar insolation was estimated.

Table 1 Selected characteristics of the research sites

Site	Latitude	Longitude	Z	α	β
S5	49°34′31.11″N	18°50′52.27″E	721.0	279	15
M1	49°34′05.12″N	18°51′28.15″E	633.3	246	18
M2	49°33′44.81″N	18°51′03.33″E	464.5	227	4

Z altitude [m AMSL], α azimuth [°]; β tilt angle [°]

Extensive, large-scale research on the water exchange balance between the atmosphere, tree stand and the soil of the Istebna spruce stands was carried out from 1997 to 2003 in the Dupniański stream catchment. Measurements were continuously taken from 22 November 1997 to 31 March 2000 and then in seasonal sessions (usually in May, July–August and September–October). Measurements were automatically taken every 6 min. Due to technical and organisational constrains of field research within tree stands, only the global solar irradiance was measured without division into its main components, i.e. direct and diffuse: site S5 at 9 m and at 0.2 m above ground, site M1 at 9 m above ground and site M2 at 9 m above ground. Global solar irradiance was gauged by precision semiconductor sensors with a spectral response from 300 to 1100 nm (the spectrum of shortwave solar radiation). Silicon sensors are insensitive to temperature variation (error less than 0.04 %/K) and have excellent long-term stability. All sensors faced upward and were placed horizontally. The cosine response for oblique rays with the field of view was approximately over 170°.

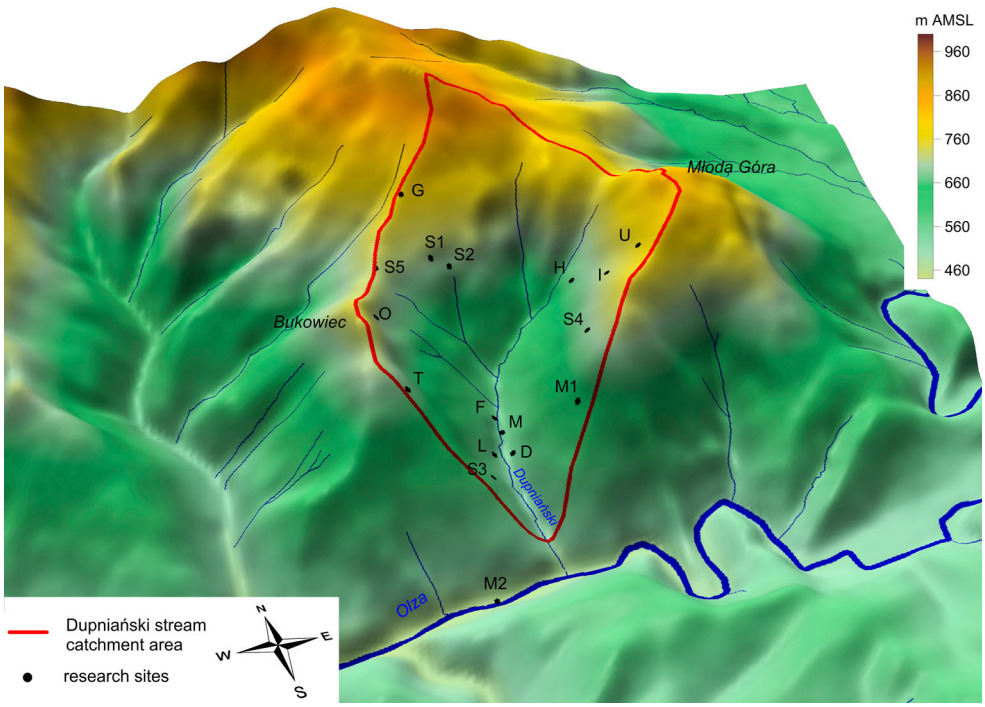

Fig. 1 Dupniański stream catchment and positions of the research sites: 14 within homogeneous, even-aged stands of different age-classes, 3 in inter-forest meadows (S5, M1 and M2)

Obstruction effect

When measurements are taken in complex terrain, and particularly in mountainous terrain, it is essential to determine the shading caused by the relief of surrounding mountain ranges, peaks and passes and the contour of adjoining tree stands. Beam solar radiation reaches the investigated surface only whilst the elevation angle of neighbouring obstructions, ε, is lower than the solar altitude angle ψ. In addition, when the horizon angles of the surrounding obstructions like mountains or tree stands are higher than 5° (Lee 2009), the diffuse radiation tilt factor, R_d, cannot be computed based on the general formula (2). In this case, it is impossible to measure the elevation angles in the field precisely; instead, estimations have to be made based on digital maps:

$$\varepsilon = \arctan\frac{\Delta Z}{d} \tag{4}$$

where ΔZ is the elevation difference between the site (the sensor) and the ridge or tree stand top blocking the sun and d defines the horizontal distance from the site (the sensor) to the ridge or tree stand top blocking the sun. The elevation differences (ΔZ) and straight-line horizontal distances (d) may be calculated in different directions from cross-section contours. In terrain which is covered with tree stands, the cross-section contours should be estimated from a digital surface model (DSM) including both terrain (digital elevation model, DEM) and the height of tree stands (digital forest elevation model, DFEM). The DEM available for the investigated area was with a scale of 1:10,000 (5 × 5 m grid resolution). The DFEM was created based on the digital forest map (DFM) which is a geometrical database that contains polygons (borders of forest compartments), lines (e.g. roads, creeks) and points. Every data cell is connected to a given forest compartment, this being a special shapefile with features and attributes which holds information about the dominant species, its age, height, diameter at breast height etc. The DFM is validated comprehensively according to an inventory of exploitation plans once every 10 years (for the study area, the latest validation was in 1997) or partially due to felling or cutting plans.

The DSM is the sum of both DEM and DFEM. That is why the DFEM has to be created based on the DEM whilst retaining the same coordinates for all grid points. The points within a given forest compartment should be determined and the value of the tree stand heights assigned to the appropriate matrix cells. It was assumed that the homogeneous, even-aged spruce stands in the study region formed a solid, uniform barrier which totally blocked solar radiation in longitudinal axis. Elevation angles were calculated based on the DSM with the area of 30 km^2 (5 × 6 km rectangle). All cross-section contours around the research site were calculated with a resolution of $\Delta\alpha = 0.25°$ (1440 profiles). Figure 2 shows four cross-section profiles in the four main directions: S-N, SW-

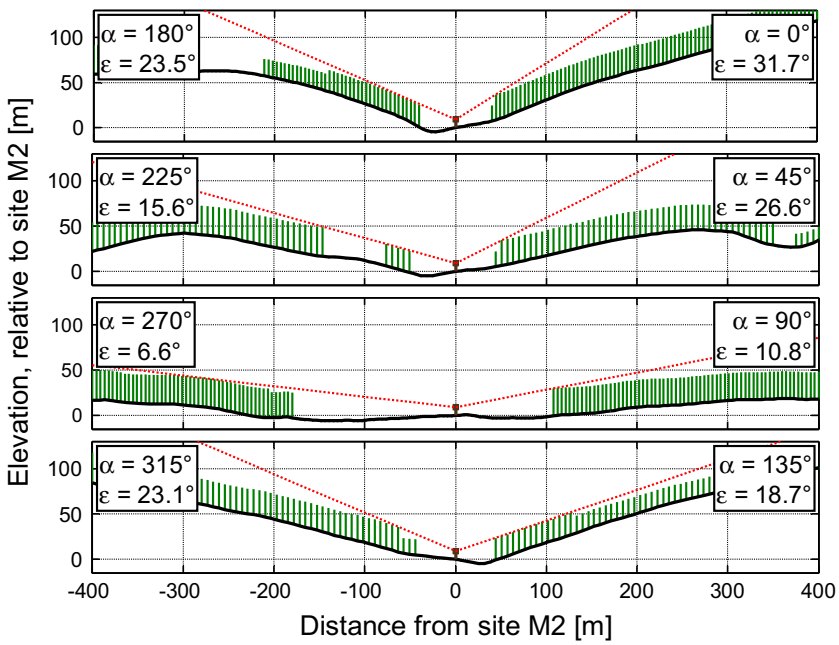

Fig. 2 The cross-section profiles of the terrain and tree stands, estimated in the four main directions, S-N, SW-NE, W-E and NW-SE, closest to site M2, located in the valley bottom (α is azimuth angle, ε is elevation angle, denoted as *dotted lines*). The elevations of the terrain and tree stands were approximated based on the digital surface model (the sum of digital elevation model and digital forest elevation model, see the text). In the all presented cases, the sky area viewed from the research plot (solar radiation sensor) was more obstructed by nearby tree stands (marked as *vertical solid short lines*) than by the relief of the surrounding terrain (*solid line*). Additionally, the elevation angles ε were considerably higher than 5°, which is the critical value acceptable by solar radiation measurement regimes

NE, W-E and NW-SE, for the research site M2, located in the valley bottom. The sky area viewed from this research plot was obstructed more by nearby tree stands than by the relief of the surrounding terrain.

According to the isotropic model, the insolation of diffuse radiation on a tilted surface depends only on how much of the sky is visible from the surface. The sky view factor, *SVF*, (Iqbal 1983) is evaluated as the ratio of the projected surface of the visible part of the hemisphere to the area of a whole hemisphere of unitary radius:

$$\mathrm{SVF} = \frac{1}{360}\int_{0}^{360}(1-\sin\varepsilon)d\alpha \tag{5}$$

where ε is elevation angle of surrounding obstructions (dependent on azimuth angle, α) and α represents azimuth. Table 2 presents the calculated values of the sky view factors at the study plots at different heights based on the generated DSM. Computed values clearly demonstrate that site M1 was the least obstructed plot (for sites situated in open fields). Site M1 was located on the westward slope in the central part of Dupniański stream valley, and approximately 79 % of the sky hemisphere was visible. Site M2, situated at the valley bottom, was the most shaded (roughly 65 % of the sky was observable). The *SVF* at site S5 varied about 8 % for the sensors positioned 9 and 0.2 m over the ground, respectively. In addition, Table 2 includes values of the SVF_{TO} evaluated taking into account only the relief of the terrain and values of the standard diffuse radiation tilt factor R_d.

Figure 3 presents direct comparisons between the calculated maximum elevation angles for all investigated sites and solar elevation angles, computed on three characteristic days: the summer solstice, the equinox and the winter solstice. It may be observed that the real sunrise and sunset ($\psi=\varepsilon$) could occur at different times than those theoretically calculated $\psi=0$ due to the obstruction effects. On the summer solstice and equinox, the real sunrise would have been about 2 h later, on average, compared to the hypothetical times for sites M1 and S5. On the other hand, sunset would have taken place earlier at the investigated sites with the exception of site S5, which was situated toward the west ($\alpha=279°$). The heaviest shading appeared on the winter solstice. There were no sunrise

Table 2 Solar radiation diversity coefficients calculated at the given height at all investigated sites in Dupniański stream valley

Site	*EABSI* [kWh m^{-2}]	$\frac{EABSI}{EABSI_{\mathrm{M1}}}$ [%]	$\Delta\overline{H}$ [%]	R_d	SVF_{TO} terrain only	*SVF*	$\frac{\mathrm{SVF}}{\mathrm{SVF_{M1}}}$ [%]	Z_t	*Z*
S5	1293.6	85.4	−3.1	0.9830	0.9489	0.7512	94.9	9.0	719.7
S5	1224.5	80.8	−8.2		0.9284	0.6744	85.2	0.2	
S5	1222.7	80.7	−8.4		0.9190	0.6727	85.0	0.0	
M1	1515.5	100.0	−0.2	0.9755	0.9118	0.7914	100.0	9.0	642.6
M1	1514.5	99.9	−0.3		0.8638	0.7447	94.1	0.0	
M2	1325.9	87.5	−10.2	0.9988	0.8243	0.6536	82.6	9.0	464.5
M2	1148.3	75.8	−22.2		0.7992	0.5263	66.5	0.0	
S1	1562.5	103.1	−9.9	0.9532		0.6776	85.6	4.0	706.0
S2	1754.8	115.8	−1.6	0.9603		0.7778	98.3	13.0	698.2
S3	1259.4	83.1	−0.8	0.9698		0.8215	103.8	38.0	556.1
S4	1311.6	86.5	−0.1	0.9755		0.8674	109.6	37.0	691.3
U	1111.6	73.3	−15.8	0.9668		0.6512	82.3	1.0	757.4
D	1233.0	81.4	−19.7	0.9755		0.4731	59.8	6.0	534.6
M	1082.8	71.4	−28.3	0.9891		0.5222	66.0	13.0	540.2
I	1318.4	87.0	−3.2	0.9698		0.7833	99.0	14.0	720.0
H	1344.5	88.7	−3.4	0.9872		0.5955	75.2	15.0	673.1
T	1676.7	110.6	−0.2	0.9830		0.7758	98.0	21.0	683.5
G	1591.4	105.0	−2.0	0.9891		0.7823	98.9	25.0	773.2
O	1430.6	94.4	−0.3	0.9636		0.8174	103.3	36.0	716.8
L	1439.5	95.0	−3.1	0.9636		0.7735	97.7	38.0	539.4
F	1339.3	88.4	−5.8	0.9938		0.7608	96.1	44.0	551.9

EABSI estimated annual beam solar insolation on tilted surface including shading of surrounding mountains and tree stands; $\Delta\overline{H}$ estimated annual loss of beam solar insolation relative to non-shaded surface; R_d diffuse radiation tilt factor, Eq. (2); SVF_{TO} sky view factor based on terrain only; *SVF* sky view factor based on terrain and tree stands, Eq. (5); Z_t elevation taken to calculation (height of mast or tree stand) [m]; *Z* altitude [m AMSL]

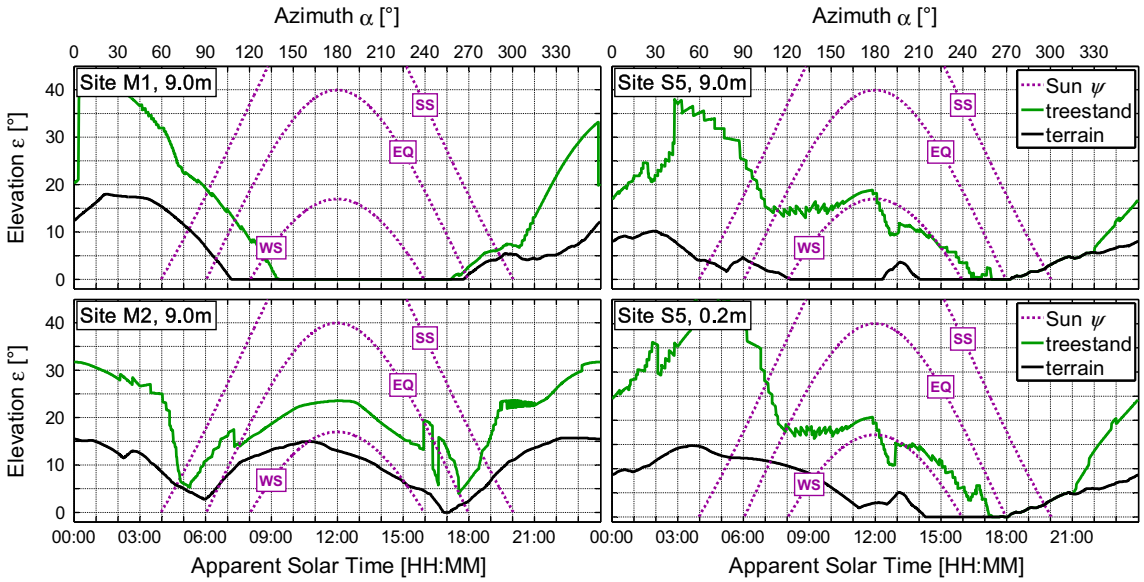

Fig. 3 Maximum elevation angles, ε, calculated for all sites situated in open fields, i.e. at inter-forest meadows, (sites S5, M1 and M2) and sun path diagrams (solar elevation angles, ψ), computed for three characteristic days in a year: the summer solstice (*SS*; about June 21st—the highest elevation of the sun for the Northern Hemisphere), the vernal/autumnal equinox (*EQ*; more or less on March 20th or September 22nd) and the winter solstice (*WS*; around December 21st—the lowest elevation of the sun for the Northern Hemisphere). It may be observed that in the presented cases the real sunrise and sunset ($\psi = \varepsilon$) generally occur at different times than the theoretically calculated ones ($\psi = 0$). On the winter solstice, due to the obstruction effect caused by the shape of adjacent tree stands as well as the surrounding slopes, there were no sunrise and sunset at site M2 at all because the beam solar radiation was completely blocked by the terrain and surrounding tree stands. A similar situation occurred at site S5, especially at 0.2 m above ground because the direct solar radiation could reach the sensors during only very briefly, from 13:00 to 14:00 apparent solar time (AST)

and sunset at site M2 at all because the beam solar radiation was completely blocked by the terrain and surrounding tree stands. A similar situation occurred at site S5. In this case, the sun's rays were attenuated by tree stands and the direct solar radiation could reach the sensors during only a very short period of time, from 13:00 to 14:00 AST. It may be also noticed that the distance in time between measurements (6 min) is equivalent of a maximum up to 1° change in the values of solar elevation angle (ψ).

Figure 4 presents diurnal patterns of global solar irradiance, recorded on a sunny day, at sites M1 and S5 on 26 June 1998. It may be observed that after theoretical sunrise (03:58 AST, $\alpha = 59.5°$) at all sites, the readings became greater than zero (diffuse radiation reached the sensors). The real sunrise at site M1, caused by the outline of adjoining tree stands ($\psi = \varepsilon = 17.1°$), would have been delayed by 2 h until 06:07 AST ($\alpha = 92°$); nonetheless, the recorded readings did not change significantly. A noteworthy increase was not detected until about 06:30 AST (the beam component of solar radiation reached the sensor). The solar altitude angle was 21° and the tree stand elevation was estimated at 15°, an error of 6°. At about 13:30 AST, the sky became a bit cloudy; hence, the moment of real sunset, caused by the contour of the adjacent tree stand, was not clearly noticeable. A small drop of irradiance was observed at about 19:16 AST, roughly 10 min later than was reckoned, and it can be assumed that at that time, the sun set behind a tree stand ($\psi = 6°$, $\varepsilon = 7°$, a difference of −1°). A similar situation was monitored at site S5 at both levels. The neighbouring tree stands delayed the real sunrise for about 2 h and 10 min at 9 m above ground (observed conformity of a theoretical estimation to the measurements). The real sunrise 0.2 m above ground was additionally delayed for 40 min. Due to low elevations of the nearest mountain range to the west ($\varepsilon \cong 2°$), the sunsets are not clearly visible in the presented diurnal patterns. After the calculated theoretical sunset at 20:01 AST, the gauged data diminished to zero.

Solar radiation variations in Dupniański stream valley

At first, solar radiation variations in the investigated region were estimated based on a series of numerical computations. The amount of solar radiation reaching the Earth's surface changes continuously over time as a result of both random atmospheric conditions as well as rotary movements of the Earth and may be described by analytical equations. The expression of the variability of diffuse radiation is based on long-term observation and developed empirical correlations. All formulae used to calculate both direct and diffuse component of solar radiation are included in Online Resource 1. Due to a lack of data on albedo changeability in the investigated area,

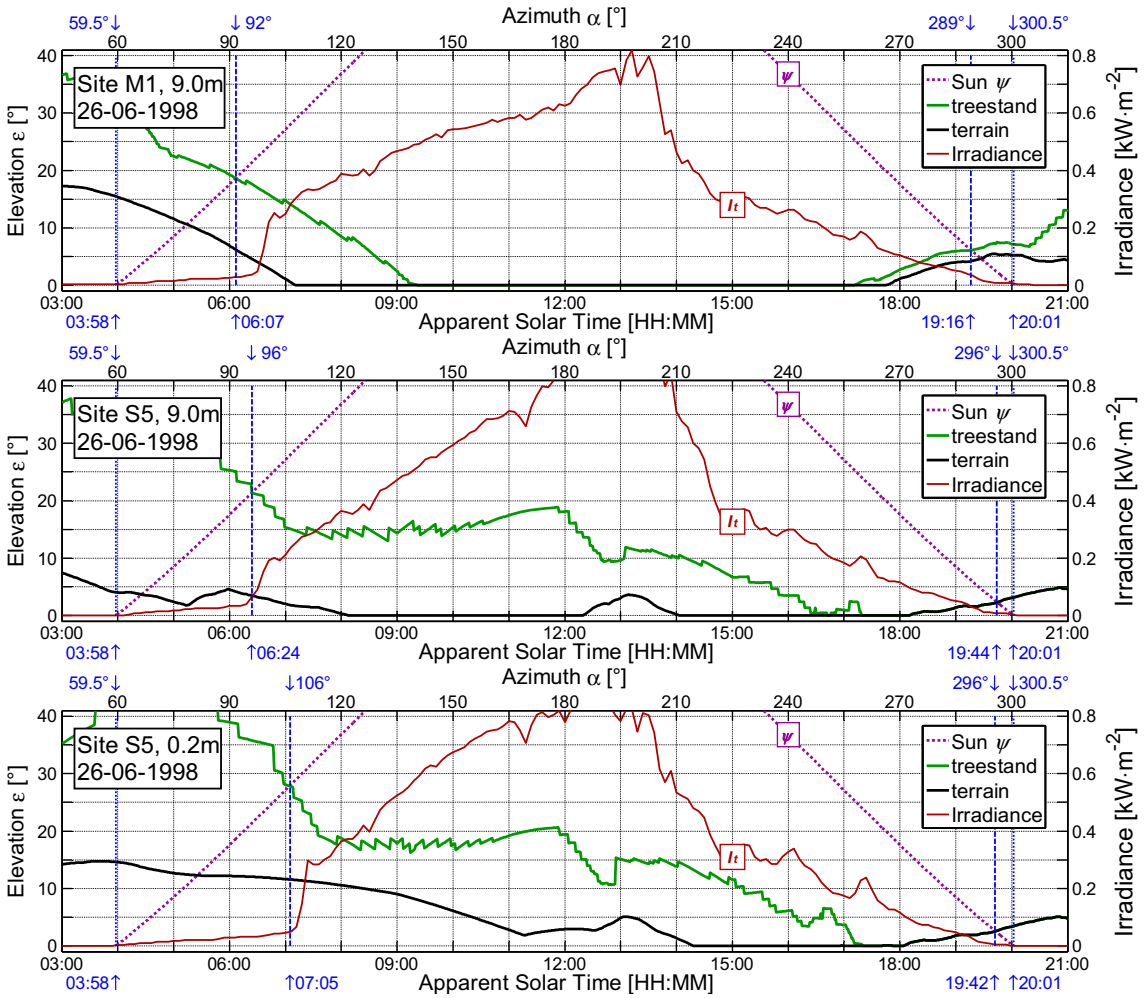

Fig. 4 Diurnal patterns of total solar irradiance, I_t, recorded during a sunny day, at sites M1 (at 9 m above ground) and S5 (at 9 and 0.2 m above ground) on 26 June 1998 (around the summer solstice). It may be observed that at all the sites after theoretical sunrise at 03:58 AST (azimuth $\alpha = 59.5°$) the readings became greater than zero (the diffuse component of solar radiation reached the solar sensors). At site M1, a significant increase of solar radiation was not recorded until 06:30 AST due to the shape of adjoining tree stands; therefore, real sunrise did not occur until this time. At site S5, the real sunrise at 0.2 m above ground was delayed for nearly 40 min, compared to the sensor mounted 9 m above ground. The real sunset times were not clearly noticeable (the sky became a bit cloudy at about 13:30 AST). After the calculated theoretical sunset at 20:01 AST, the gauged data diminished to zero

the reflected component of total insolation was omitted ($I_{r\beta}=0$).

The beam radiation tilt factor can be estimated by numerical integration of the numerator and the denominator in Eq. (3) (Pluta 2000). In mountainous terrain, it is necessary to take into consideration the obstruction effect. In order to define the obstruction effect, the temporary shading vector (*TSV*) may be defined as follows:

$$\mathrm{TSV} = \begin{cases} 1 & \psi > \varepsilon \wedge \cos\theta \geq 0 \\ 0 & \psi \leq \varepsilon \vee \cos\theta < 0 \end{cases} \tag{6}$$

where θ is incidence angle of the direct solar radiation component to the investigated surface. The coefficient TSV includes information about temporary shading caused by surrounding mountain ranges and tree stands as well as differences in sunrise and sunset resulting from the aspect and tilt angle of the investigated surface. Therefore, the beam shading factor, equivalent to R_b for unobstructed surfaces, may be calculated for an inclined surface as follows

$$\mathrm{BSF}_{\beta,h} = \frac{\int^{\mathrm{day}} I_b \cdot \mathrm{TSV}_\beta \cdot \cos\theta_\beta d\omega}{\int^{\mathrm{day}} I_b \cdot \cos\theta_h d\omega} \tag{7}$$

where $BSF_{\beta,h}$ is beam shading factor for a tilted surface, daily mean. Numerical integration in Eq. (7) was carried out based on Newton–Cotes quadrature rules of the first order ($N=1440$). Fig. ESM2-1 in Online Resource 2

presents annual changeability of coefficients $BSF_{\beta,h}$ and R_b ($BSF_{\beta,h}=R_b$ for $TSV_\beta \equiv 1$) computed for all research sites at the study area (for sites located in open fields: M1, M2 and S5 at ground level, for other sites at the height of tree stand tops at the given site).

Table 2 displays the estimated annual beam solar radiation on tilted surfaces including the shading effect, $EABSI = \int^{\text{year}} I_b \cos\theta_\beta dt$ [kWh m^{-2}] and the approximated annual loss of beam solar insolation caused by shading effect ($\Delta\overline{H}$ [%]) compared to a theoretical unobstructed surface situated in the same place. The annual loss was extremely dependent on the elevation over the ground as well as over the valley bottom. The change of elevation from 9 m to ground level caused a loss of more than 5 % for site S5 (placed high in the valley) and around 12 % for site M2 (in the valley bottom). The highest loss of direct insolation was observed at site M ($\Delta\overline{H} = -28.3\%$), situated in the valley bottom near site D ($\Delta\overline{H} = -20\%$). Although all sites in the research area were shaded, the obstruction effect happened primarily in winter (lower values of direct irradiance compared to summer); therefore, sites with tall tree stands (like for instance S4, T and O) were characterised by the lowest, practically negligible, annual loss of beam insolation.

The coefficients R_d and SVF, calculated based on Eq. (2) and (5) for all study plots, are presented in Table 2. These factors depended on the topographical relief of adjoining terrain and the contour of neighbouring tree stands only. The validation of SVF values should have been done at the same time as the forest management plan was updated due to silvicultural practices and the annual growth of tree stands.

The daily mean solar insolation reaching densely forested slopes in Dupniański stream valley, H_β, may be estimated by the equation:

$$H_\beta = BSF_{\beta,h}\cdot\left(K_T\cdot H_0 - H_{d,h}\right) + \text{SVF}\cdot H_{d,h} \tag{8}$$

where $H_{d,h}$ is daily mean insolation of the diffuse component on a horizontal surface and H_0 is daily average total insolation on an extraterrestrial horizontal surface (Online Resource 1). Example, theoretical calculations were performed for the winter solstice, the equinox and the summer solstice for different sky conditions based on Iqbal's (1983) classification ($K_T=0.1$ cloudy sky day, $K_T=0.4$ partially cloudy sky day, $K_T=0.7$ clear sky day). The results are shown in Fig. ESM2-2 in Online Resource 2. Under an overcast sky when diffuse radiation was the dominant component, the variability of solar insolation directly depended on the values of SVF. The beam shading factor primarily affected solar insolation under a clear sky. The values of $BSF_{\beta,h}$ demonstrated seasonal changeability (Fig. ESM2-1 in Online Resource 2) and largely depended on the aspect and tilt angle of the investigated surface. This is why the variability was very high in winter (from 0.1 kWh m^{-2} at site M2 to 3.3 kWh m^{-2} at site S2, for $K_T=0.1$). In summer, the variability was moderately low (from 6.1 kWh m^{-2} at site M to 8.1 kWh m^{-2} at site T, for $K_T=0.7$).

Taking aforementioned numerical simulations into consideration, it is possible to develop an empirical model of the solar insolation reaching a given horizontal surface within the research valley. Based on recorded data, daily mean values of global insolation were calculated. All investigated surfaces where measurements were taken were obstructed; therefore, it may be expected that the model equation should be based on the estimated SVF from the DSM. Additionally, based on theoretical assumptions and computations presented in Online Resource 3, a simply linear model may be used. It can be noticed (Fig. ESM3-2 in Online Resource 3) that the slope coefficients were proportional to the SVF ratio for a given surface and also to the SVF for the reference surface at the least obstructed site (M1):

$$H_i = p\cdot\frac{\text{SVF}_i}{\text{SVF}_{\text{M1}}}\cdot H_{\text{M1}} \tag{9}$$

where H_i is daily mean global solar insolation on a horizontal surface at a given research site calculated based on recorded data, SVF_i is sky view factor for a given research site, H_{M1} is daily mean total insolation on a horizontal surface at site M1 calculated based on recorded data, the least obstructed site, and SVF_{M1} is the sky view factor for site M1. The relationship between solar insolation recorded at different sites is presented in Fig. 5. To reduce the influence of random weather conditions at research sites, only data which matched the condition $0.5\cdot H_{\text{M1}} \le H_i \le 1.5\cdot H_{\text{M1}}$ were taken into consideration. The results of the identification of the formula (9) are presented in Table 3. The regression statistics confirm that the form of Eq. (9) was correctly matched, and according to values of the correlation coefficient R or $100\cdot R^2$, the variability of solar insolation on horizontal surfaces may be explained with good accuracy (92 %). Large values of an average error of estimation (22 %) may be explained by the measurement conditions. A sufficient number of cases used in the identification ($K>1100$) came from only three research sites; therefore, the variations in shading effect, defined by SVF, were relatively small. Additionally, the measured total solar radiation was biased due to varying weather conditions.

Discussion

The obtained results undoubtedly proved the major role played by the topographical relief of adjoining mountain ranges and above all the outline of neighbouring tree stands

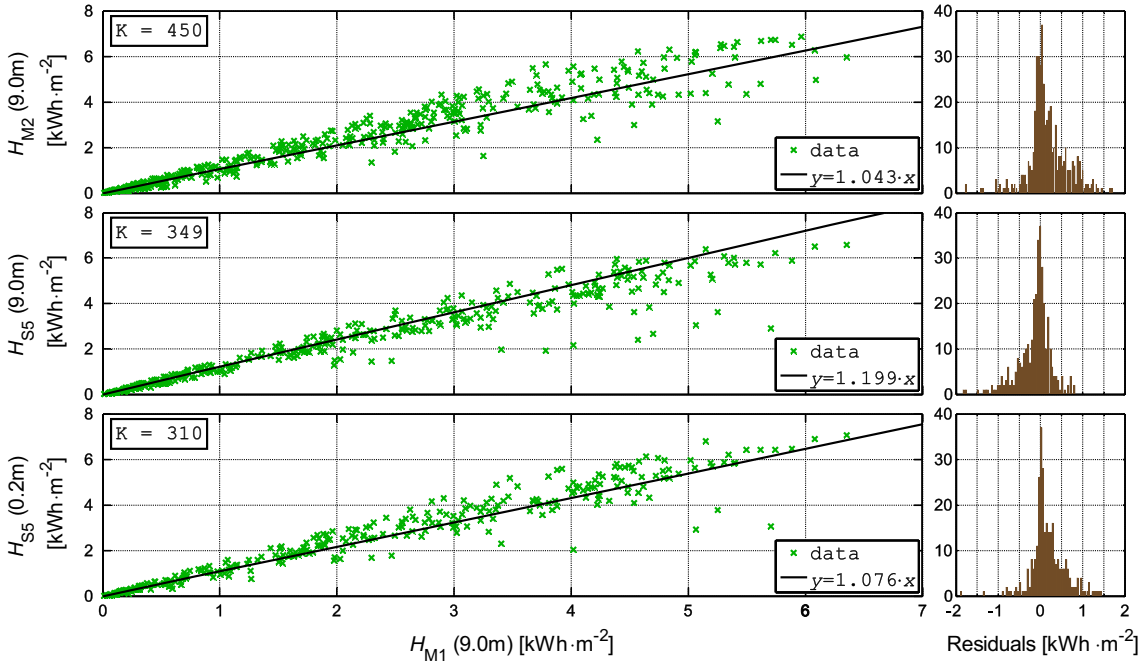

Fig. 5 Relationships between daily insolation on horizontal surfaces gauged at different sites in open fields, relative to the least obstructed site M1 with histograms of residuals (*right*). *K* number of cases, i.e. number of days used in estimation

in modelling the variability of solar insolation in a V-shaped small valley. The presented simplified empirical model provides an accurate description of the variability of solar insolation reaching spruce stands. However, due to technical conditions, solar insolation data were obtained at just three obstructed sites (four sensors at three accessible open space areas in the investigated basin). Although this was sufficient to distinguish some differences, the range of the explaining variable *SVF* was relatively small. Furthermore, readings differed significantly even if logged at the same time, due to the distances between sites (straight-line distances: S5-M1 850 m, S5-M2 1465 m, M1-M2 1010 m). Even though solar radiation was very diurnally dependent, it also demonstrated random attributes resulting from local meteorological conditions, for instance variable cloud cover, local mist and fog patches. The best solution would have been to precisely measure all components of solar radiation, using for example modern sun trackers, over the tree crowns at more study plots, not only in the inter-forest meadows, and model gauged data for all components of solar radiation separately. Such sophisticated measurements are not always possible due to technical and organisational reasons. The research valley was 95 % densely forested with only one open field which was the location of site M1. Additional open field sites S5 and M2 were, from a formal perspective, situated just near the basin border, outside the study area. It was technically impossible to position a research site or even a data logger with a solar sensor, at the summit of the dominant, unobstructed Kiczory Peak (990 m AMSL, Fig. 1). Such an additional survey on noticeably less obstructed terrain with a considerably higher *SVF* would have probably made it possible to construct a more accurate empirical model. It should be emphasised that commonly used empirical formulae which take into account the clearness index K_T cannot be straightforwardly adopted as such equations may be applied only to those regions for which they have been proposed and, above all, where data were captured in unobstructed places. In a V-shaped valley the proportions between solar radiation components may be different.

The amount of beam solar radiation reaching valley slopes was highly dependent on the topography of the immediate neighbourhood and may be determined by the $BSF_{\beta,h}$. This was clearly noticeably at site M2, which was situated at a small inter-forest meadow in the valley bottom. The lack of shading impact on the beam component was observed in June only, when the sun reached its highest point (Fig. ESM2-1 in Online Resources 2). In winter, from late November to the end of February, the beam component of solar radiation did not fall on this site, with the sun's disk taking less than 2 weeks to be completely hidden behind the densely forested mountain range, positioned to the south of the site (Fig. 1). Because of such obstructions, there were similar conditions at site S5, where in winter, the amount of beam irradiance was reduced to approximately 30 %. An analogous situation was noticed at sites U and I, located high on the western slopes of Mała Góra Mountain, as well as at site D at the bottom of the Dupniański stream valley. Tree stands at sites U and D were heavily

Table 3 Goodness-of-fit statistics for model (9)

Site	K	p	$p \cdot \frac{SVF_i}{SVF_{M1}}$	95 % CI	R	$100 \cdot R^2$	σ	μ
M2 (9.0m)	450	1.263	1.043	1.249–1.277	0.957	91.6	0.54	22.57
S5 (9.0m)	349	$K = 1109$	1.199					
S5 (0.2m)	310		1.076					

K number of cases, i.e. number of days used in estimation; p regression coefficient; *SVF* sky view factor; CI confidence intervals; R correlation coefficient; σ standard deviation of estimation; μ average error of estimation

shaded by old, mature stands with heights from 35 to 39 m. The beam component at site U was reduced by nearly 60 % from early autumn to late spring and in winter time (from December to February), whilst at site I, the loss occurred mainly in winter. At the other sites, due to the height of the overgrowing tree stands and the lack of high mountain ranges in the immediate neighbourhood, losses were not clearly observed. Obstruction of the sun's disk happened mostly just after sunrise or just before sunset, when the irradiance of the beam solar radiation was relatively small.

Seasonal changeability of coefficients $BSF_{\beta,h}$ and R_b (Fig. ESM2-1 in Online Resources 2) largely depended on the altitude of the sun as well as the aspect and the tilt angle of the investigated surface. The highest variability of the R_b was observed at sites S2, S1, T and G, as these had an aspect angle closest to the south. Site S2 ($\alpha = 189°$, 13-m-high timber pole stand) absorbed most energy in winter. The large differences between R_b and $BSF_{\beta,h}$ can be observed at sites situated in thickets (S1, U and I) and at the bottom of Dupniański stream valley (M and D). On the winter solstice, the tree stand at site S1 could absorb roughly 2.27 times more energy from beam radiation (R_b) than a horizontal surface located in the same place. Nevertheless, taking into account the obstruction effect, the gain equals 1.6× ($BSF_{\beta,h}$, Fig. ESM2-1 in Online Resources 2). In winter, tree stands at sites D and M could absorb 50 % less direct solar energy as a result of the values of cosine of the incidence angle ($\cos\theta_\beta$).

The variability of the diffuse radiation tilt factor, R_d, which only took into account the inclination angle was very low (about 2 % for sites located in open fields and approx. 4 % for all sites, Table 2) and cannot be used to describe the variability of diffuse solar radiation at the study area. Additionally, the elevation angles of the surrounding obstructions were considerable higher than 5° (Fig. 3); thus, the general formula (2) should not be implemented (Lee 2009). Computations based on the DEM only (only the relief of the terrain) could have led to the improper conclusion that the higher the altitude of the research site, the greater the part of the hemisphere that was visible (Table 2). Secondly, the standard values of R_d incorrectly indicated that the most open study plot was site M2 (Table 2), placed in the valley bottom on the least steep slope ($\beta = 4°$).

The value of *SVF* based on the DSM changed from almost 47 % at site D (thicket) to approximately 87 % at site S4 (mature tree stand). The influence of the obstruction effect is clearly noticeable at sites situated in inter-forest meadows (Table 2). A change of elevation from 9 m (the height of a mast) to ground level caused a fall in *SVF* of 16 % for site M2 (located in the valley bottom), 6 and 8 % for sites M1 and S5, respectively. The computations also showed that the highest amount of diffuse radiation was absorbed by high, mature stands at sites S3, S4 and O (*SVF* > 80%). The lowest values of *SVF* were calculated for sites D and M, approximately 47 and 52 %, respectively (Table 2). These sites were situated in the valley bottom (Fig. 1) in a 6-m-high thicket (site D) and in a 13-m-high timber pole stand (site M) and were surrounded by tall tree stands (heights of 27, 38 and 39 m). The *SVF* values for sites L and F (mature stands with heights of 38 and 44 m, respectively), which were placed in the immediate neighbourhood of sites D and M, equalled almost 77 and 76 %, respectively. A similar situation was found at site U in a 1-m-high natural regeneration, located high on the western slopes of Mała Góra Mountain. The stand in this site was also obstructed by mature seed tree stands with heights from 35 to 39 m; therefore, the sky view factor was 65 %.

Another issue worth investigating is the accuracy of both the DEM and the DFM which were used to generate the DSM and determine elevation angles and *SVF*—an input variable in the presented model. Only the height of the main crop in a given compartment was taken into account, but there were some small admixtures containing both taller and shorter stands with different structures in some logging units. Furthermore, the geometrical quality of the DFM based on orthophotomaps is usually poor. Displacements of the tree crown location, which often is the natural indicator of forest compartment borders, could reach many metres. This problem occurs especially for tall trees growing on steep slopes (Wężyk et al. 2013). Additionally, during the research, silvicultural practices were performed in the study area resulting in canopy openings or relocations of the forest walls. The biometric features of tree stands also changed continually, especially tree stand heights, due to annual growth: from 0.6–0.9 m in the second age class maturing stands (20–40 years old) to 0.3 m in the oldest mature seed stands (over 100 years

old). The DFM does not include such changes resulting from the current annual crop growth or silvicultural practices (felling and regeneration), which take several years and cause variations in height of the homogeneous structure of tree stands in logging units. What is more, the site quality index may change within one logging unit, resulting in varying heights of the dominant crop through a given section. The abovementioned problems may be nowadays solved by using modern remote sensing techniques like for instance airborne laser scanning. Such methods can provide precise information about terrain elevation, structure of vegetation, a position and height of every individual tree in the research area (Wężyk et al. 2013).

A thorough understanding of the impact of hydrometeorological factors on the water exchange balance within forest complexes would considerably expand the capability for predicting the results of silvicultural measures as well as the estimation of site productivity, which determines the growth of tree stands and forest succession. The presence of spruce stands in the study area was quite phenomenal as in this temperate climate zone spruce stands are only generally found in the higher montane zone above 1100 m AMSL. In summer, the observed and predicted diversity of solar insolation was rather low (Fig. ESM2-2 in Online Resource 2); thus, growth was fast at all sites (i.e. tree stands). In winter, the differences were significantly higher but with relatively lower global insolation. It may be suggested that the obstruction effect caused by the shape of surrounding mountain ranges lowered the annual mean temperature and made it similar to the values in the higher montane zone. Consequently, vegetation conditions at the study area were different to those usually found in the foothills (up to 600 m AMSL) and in the lower montane zone (from 600 to 1100 m AMSL). The best quality Istebna spruce stands with heights up to 44 m covered the eastward slopes of the Dupniański stream valley (sites L and F, Fig. 1).

Linear models or segment piecewise linear regressions are often used in solar engineering. Based on presented methodology, the simplified empirical model takes into account the well-known sky view factor only. It should be noted that the numerically estimated slope coefficient p in the model equation probably represents some features of the valley shape and ought to be evaluated separately for each valley or investigated terrain. Furthermore, it may be expected that the slope coefficient p also may include information about the reflected component. The impact of snow cover (with a reflection coefficient of 0.9) on the presence of reflected solar radiation in global insolation is presented in Online Resource 4.

Conclusions

A significant question arises over whether this simple analytical description can have a more general character and may concern terrains with a more complex structure. It may be expected that a general model formula should be based on a segment piecewise regression (Fig. ESM3–4 and Fig. ESM3–5 in Online Resource 3). Probably, a two-segment piecewise linear regression could be sufficient to solve this task and an intersection point should be dependent upon the moment (equivalent to insolation on an unobstructed site) when the sun's disk is completely hidden behind obstructions. The investigated region was covered by dense homogenous coniferous stands and solar radiation was strongly attenuated within canopies. It would be also essential to investigate suppression of solar radiation inside tree stands and its influence on the values of SVF or $BSF_{\beta.h}$. More complicated conditions may appear in terrain forested by deciduous stands whose foliage changes seasonally (Holst et al. 2004); hence, the SVF and $BSF_{\beta.h}$ would also indicate annual changeability. Under such conditions, the sun's disk may be visible through a stem or crown layer. Nevertheless, this situation usually may occur when solar altitude angles are very low with little solar irradiance (mostly just after sunrise or just before sunset); thus, possible divergences might simply be neglected. The necessary improvements may be possible after a series of sophisticated measurements of solar radiation components taken within various types of terrain.

Acknowledgments Funding support for this research was provided by National Science Centre (NCN), Poland (Award No. N N309 427338).

References

Bouchter J-F, Bernier PY, Munson AD (2001) Radiation and soil temperature interactions on the growth and physiology of eastern white pine (*Pinus strobus* L.) seedlings. Plant Soil 236: 165–174

Chen JM, Blanken PD, Black TA, Guilbeault M, Chen S (1997) Radiation regime and canopy architecture in a boreal aspen forest. Agric For Meteorol 86(1–2):107–125

Coops NC, Waring RH, Moncrieff JB (2000) Estimating mean monthly incident solar radiation on horizontal and inclined slopes from mean monthly temperatures extremes. Int J Biometeorol 44:204–211

Duffie JA, Beckman WA (1991) Solar engineering of thermal processes. Willey, New York

Dziadowiec H, Pokojska U, Prusinkiewicz Z (2004) Materia organiczna, koloidy i roztwór glebowy jako przedmiot badan ´ specjalistycznych. In: Bednarek R, Dziadowiec H, Pokojska U, Prusinkiewicz Z (eds) Badania Ekologiczno-gleboznawcze. PWN, Warszawa, pp. 113–245

Ediriweera S, Singhakumara BMP, Ashton MS (2008) Variation in canopy structure, light and soil nutrition across elevation of a Sri Lankan tropical rain forest. For Ecol Manag 256:1339–1349

Galicia L, López-Blanco J, Zarco-Arista AE, Filips V, García-Oliva F (1999) The relationship between solar radiation interception and soil water content in a tropical deciduous forest in Mexico. Catena 36(1–2):153–164

Grayson SF, Buckley DS, Henning JG, Schweitzer CJ, Gottschalk KW, Loftis DL (2012) Understory light regimes following silvicultural treatments in central hardwood forests in Kentucky, USA. For Ecol Manag 279:66–76

Holst T, Mayer H (2005) Radiation components of beech stands in Southwest Germany. Meteorol Z 14:107–115

Holst T, Hauser S, Kirchgäßner A, Matzarakis A, Mayer H, Schindler D (2004) Measuring and modelling plant area index in beech stands. Int J Biometeorol 48:192–201

Holst T, Rost J, Mayer H (2005) Net radiation balance for two forested slopes on opposite sides of a valley. Int J Biometeorol 49:275–284. doi:10.1007/s00484-004-0251-1

Iqbal M (1983) An introduction to solar radiation. Academic Press, Toronto

Lee C (2009) An overview of the requirements and operational issues, derived from the BSRN. Operations manual version 2.1. Kipp & Zonen. http://www.kippzonen.com/Download/124/Scientific-Solar-Monitoring-Station-BSRN-requirements

Liu BYH, Jordan RC (1963) The long term average performance of flat-plate solar-energy collectors. Sol Energy 7:53

Mayer H, Holst T, Schindler D (2002) Microclimate within beech stands—part I: photo-synthetically active radiation. Forstwiss Centralbl 121:301–321 (in German)

Piedallu C, Gégout J-C (2008) Efficient assessment of topographic solar radiation to improve plant distribution models. Agric For Meteorol 148(11):1696–1706

Pluta Z (2000) Podstawy teoretyczne fototermicznej konwersji energii słonecznej. Oficyna Wydawnicza Politechniki Warszawskiej, Warszawa

Pons TL (2000) Seed responses to light. In: Fenner M (ed) Seeds, the ecology of regeneration in plant communities, 2nd edn. C.A.B. International, Wallingford, pp. 237–260

Promis A, Schindler D, Reif A, Cruz G (2009) Solar radiation transmission in and around canopy gaps in an uneven-aged Nothofagus betuloides forest. Int J Biometeorol 53:355–367. doi:10.1007/s00484-009-0222-7

Puchalski T, Prusinkiewicz Z (1975) Ekologiczne podstawy siedliskoznawstwa leśnego. PWRiL, Warszawa

Şen Z (2008) Solar energy fundamentals and modeling techniques: atmosphere, environment, climate change and renewable energy. Springer-Verlag London Ltd, London

Tajchman SJ (1984) Distribution of the radiative index of dryness and forest site quality in a mountainous watershed. Can J For Res 14(5): 717–721

Tian YQ, Davies-Colley RJ, Gong P, Thorrold BW (2001) Estimating solar radiation on slopes of arbitrary aspect. Agric For Meteorol 109: 67–74

Vose J, Allen H L (1988) Leaf area, stemwood growth, and nutrition relationships in loblolly pine. For Sci 34:547–563

Wang Q, Tenhunen J, Schmidt M, Kolcun O, Droesler M, Reichstein M (2006) Estimation of total, direct and diffuse PAR under clear skies in complex alpine terrain of the National Park Berchtesgaden, Germany. Ecol Model 196(1–2):149–162

Wężyk P, Szostak M, Tompalski P (2013) Use of airborne laser scanning data for a revision and update of a digital forest map and its descriptive database: a case study from the Tatra National Park. In: Kozak J et al. (eds) The carpathians: integrating nature and society towards sustainability, environmental science and engineering. Springer-Verlag, Berlin

Wilson KB, Hanson PJ, Baldocchi DD (2000) Factors controlling evaporation and energy partitioning beneath a deciduous forest over an annual cycle. Agric For Meteorol 102:83–103. doi:10.1016/S0168-1923(00)00124-6

Yard MD, Bennett GE, Mietz SN, Coggins LG Jr, Stevens LE, Hueftle S, Blinn DW (2005) Influence of topographic complexity on solar insolation estimates for the Colorado River, Grand Canyon, AZ. Ecol Model 183:157–172